Exploring Halo Substructure with Giant Stars: A diffuse star cloud or tidal debris around the Milky Way in Triangulum-Andromeda

Helio J. Rocha-Pinto, Steven R. Majewski, M. F. Skrutskie, Jeffrey D. Crane, Richard J. Patterson

Department of Astronomy, University of Virginia, Charlottesville, VA 22903

helio, srm4n, mfs4n, jdc2k, rjp0i@virginia.edu

ABSTRACT

We report here the discovery of an apparent excess of 2MASS M giant candidates with dereddened $0.85 < J - K_S < 1.2$ spanning a considerably large area of the celestial sphere between, at least, $100^\circ < l < 150^\circ$ and $-20^\circ > b > -40^\circ$, and covering most of the constellations of Triangulum and Andromeda. This structure does not seem to be preferentially distributed around a clear core, but rather lies in a tenuous, clumpy cloud-like structure tens of kiloparsecs away. The reduced proper-motion diagram as well as spectroscopy of a subsample shows these excess stars to be real giants, not contaminating dwarfs. Radial velocity measurements indicate among those M giants the presence of a coherent kinematical structure with a velocity dispersion $\sigma < 17$ km s^{-1}. Our findings support the existence of a quite dispersed stellar structure around the Milky Way that, due to its coreless and sparse distribution, could be part of a tidal stream or a new kind of satellite galaxy.

Subject headings: Galaxy: structure – Galaxy: disk – galaxies: interactions

1. Introduction

Recent surveys of the Galactic stellar content (e.g., Ibata et al. 1994, 2002; Majewski et al. 1996, 2003, hereafter M03; Newberg et al. 2002, hereafter N02) have consolidated the notion that galactic mergers play a fundamental role in building our Milky Way (MW). A prominent feature in the Galactic halo is the tidal stream of the Sagittarius dSph, which circles the MW in a nearly polar orbit (Ibata et al. 2001, M03). Another companion of our Galaxy remained hidden behind the veil of MW disk stars until its debris was discovered by

N02 as an overdensity of A-F dwarfs in Monoceros. By using a statistical method to find relative stellar distances for a population with unknown [Fe/H], Rocha-Pinto et al. (2003, hereafter R03) found M giants from this disrupted satellite galaxy distributed over a large area of sky (see also M03). Given the evidence that the MW halo is highly substructured (Majewski 2003, e.g.), it is likely that additional companions of the Milky Way remain to be discovered (Willman et al. 2004, see also).

In the investigation of the N02 tidal stream, R03 pointed out smaller, more distant ($R_{GC} > 20$ kpc) M giant overdensities that did not seem to be part of that structure. We have undertaken a systematic investigation of two of these more distant overdensities using a larger subsample of 2MASS M giant candidates. Here we show that at least one of these more distant M giants constitutes part of a new coherent structure that spans at least $50^\circ \times 20^\circ$ in the second Galactic quadrant, over much of the constellations of Triangulum and Andromeda.

2. Data

The stellar sample we explore includes all stars from the 2MASS Point Source Release (2MASS-PSR) having dereddened colors $0.85 < J - K_S < 1.5$, $K_S < 13.0$ and photometric quality flag '`AAA`' that also meet the color selection criteria for M giants candidates in the $(J - K_S, J - H)$ diagram (M03). Reddening and extinction in J and K_S were calculated by $(A_J, A_{K_S}, E_{J-K_S}) = (0.90, 0.25, 0.65)\alpha E_{B-V}$, where E_{B-V} is from Schlegel et al. (1998). α is an attenuation factor that produces better results when using the Schlegel et al. E_{B-V} in regions of high extinction. The adopted value of $\alpha = \frac{2}{3}$, as well as the selected extinction coefficients at J and K_S, best reconstructed the un-extinguished distribution of normal giants in the $(J - K_S, J - H)$ diagram when applied to raw 2MASS J, H, and K_S magnitudes in regions of moderate extinction ($A_V \sim 3$).

Relative stellar distances were calculated as in R03: The distance probability density function (DPDF) for each star is computed by propagating the uncertainty of the stellar metallicity, according to an assumed metallicity probability distribution function (MPDF). To facilitate comparison with the R03 distance scale, we adopt a Gaussian MPDF, with $\langle$[Fe/H]$\rangle = -1.00$ dex and $\sigma = 0.40$ dex. Hereafter, we will use as an estimate of the distance the mode of the DPDF for each star. R03 give an approximate equation for the variation of this distance as a function of [Fe/H].

3. An Excess of Stars in the Outer Galaxy

The Galactic Equator and $l = 0, 180^{\circ}$ meridian can be used in the definition of three presumed MW symmetries, namely, equatorial, meridional and diagonal, defined so that a stellar field limited by the coordinates $([l_1 : l_2], [b_1 : b_2])$ has as analogs the fields $([l_1 : l_2], [-b_1 : -b_2])$, $([-l_1 : -l_2], [b_1 : b_2])$ and $([-l_1 : -l_2], [-b_1 : -b_2])$, respectively. We compare these pairs of analogous fields to search for *asymmetries* in stellar density that may represent Galactic substructure. We discard from the analysis any 1 deg^2 field if it, or its counterpart, has $E_{B-V} > 0.15$. This reddening limit ensures that the differential reddening among the target fields is $A_{K_S} \leq 0.03$.

Figure 1a summarizes this symmetry analysis in a composite polar contour plot of excess stars in the Galactic neighborhood. The densities correspond to the positive excesses in stellar density between opposite hemispheres across each symmetry, averaged over the three symmetries considered above.

Several features in the plot can be identified with known satellites of the Milky Way, reinforcing our claim that we recover significant halo substructures with this method. The precise distance range where these structures make their appearance in the plot is not accurate for some satellites because distances were calculated for a population with $\langle$[Fe/H]$\rangle = -1.0 \pm 0.4$. Residual photometric errors, metallicity spread and extinction effects artificially stretch the distance range covered by these structures, giving rise to "Finger of God" effects. Pieces of the extensive tidal tail structure that in our previous papers we dubbed the Galactic Anticenter Stellar Structure (GASS) — associated with N02's discovery in Monoceros — are seen in Figure 1a at $110^{\circ} < l < 170^{\circ}$ and $210^{\circ} < l < 270^{\circ}$ with heliocentric distances between 5 and 13 kpc. In this plot, GASS's signal is not very strong nor does it appear as a continuous stream (as in R03) due to the severe limit on $E(B-V)$ adopted.

Here we call attention to an additional, unexplained, large grouping of apparent M giants stretching from $l \sim 100^{\circ}$ to $l \sim 150^{\circ}$ between 15 to 30 kpc from the Sun. Two areas of higher density are in the constellations Triangulum and Andromeda (hereafter, "TriAnd"). Another grouping (hereafter, "Per"), at $155^{\circ} < l < 174^{\circ}$ and $d \gtrsim 18$ kpc, lies in Perseus. The latter group is more easily seen in Figure 1b, when we apply a less rigorous reddening limit. Both panels give the impression that Per is related to TriAnd, but, as shown below, they are likely to be unrelated. These same concentrations were already found by R03 as secondary peaks within the DPDF at the corresponding lines of sight.

Figure 2 presents an on-sky projection of the residual density of M giant candidates having $15 < d < 40$ kpc in the TriAnd area, averaged over the three Galactic symmetries. The figure shows the clear asymmetry in the M giant distribution across the Galactic plane,

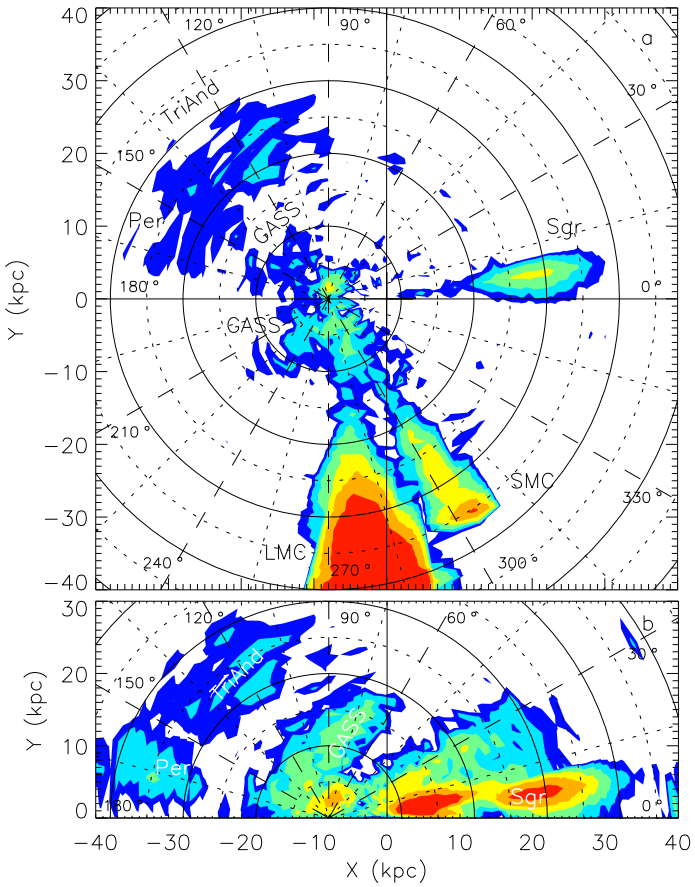

Fig. 1.— Excess stars in the Milky Way vicinity. (a) Polar contour plot (circles centered on the Sun) showing the density of excess stars projected onto the Galactic plane. Contour levels represent, at $R_{GC} \sim 30$ kpc, densities of nearly 10, 20, 40, 80, 160 and 320 stars kpc^{-2}. Most of the stellar overdensities correspond to known Milky Way satellites — the LMC, SMC, and Sagittarius galaxies — or an extension of the recently system first discovered in Monoceros by N02, labeled GASS (Galactic Anticenter Stellar Stream) in the plot. A new, large area overdensity of stars, here called TriAnd, can be seen between 15 and 30 kpc from the Sun, between the longitudes $l \sim 100°$ and $l \sim 170°$. (b) Expanded view of the TriAnd region when R03's reddening limit of $E_{B-V} < 0.55$ is adopted. Per was initially found when we limited the sample to this reddening value. With a more conservative reddening limit, Per is mostly eliminated as an excess feature. We opted to include its stars in this discussion to test the possibility that Per and TriAnd are associated.

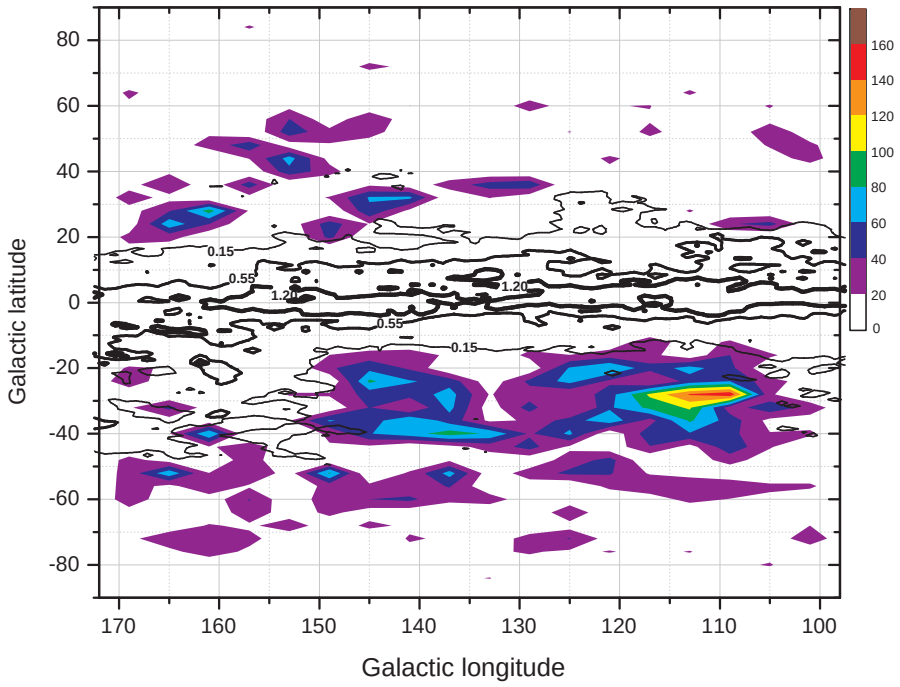

Fig. 2.— 2MASS M giant candidate overdensity having $0.85 < J - K_S \leq 1.50$, $K_S < 13.0$, $15 < d < 40$ kpc and $E_{B-V} < 0.15$ in the region of Triangulum and Andromeda, averaged over the three Galactic symmetries. Unshaded contour levels show the average reddening in this sky field at $E_{B-V} = 0.15$, 0.55 and 1.20. The other concentration considered in this work, in Perseus, centered at $(l, b) = (163°, -20°)$, is not shown in this plot, due to the conservative reddening limited adopted.

however, as in Figure 1, this projection shows no obvious core as would be expected for a typical dwarf galaxy. The presence of considerable foreground dust may hinder the search for a core in this region, as can be appreciated from the large open areas that we have been forced to ignore due to excessive reddening.

We have considered the possibility that TriAnd is an artifact created by misclassified M dwarfs. The separation between M giants and dwarfs in the $(J-K_S, J-H)$ diagram begins at $J-K_S \sim 0.85$ (Bessell & Brett 1988), so we expect some interloping dwarfs at the blue limit of our sample, due to photometric errors and cosmic scatter. Indeed, we have found in our data a kind of shell around the Sun, along almost every line of sight, composed of stars having $0.85 < J-K_S < 0.90$ and $12.5 < K_S < 13.0$, which we take to be misclassified M dwarfs (see discussion of a similar "contamination shell" effect in M03). The apparent magnitudes of these shell interlopers are translated to similar stellar distances as redder, intrinsically brighter TriAnd M giants. While a *symmetric* shell of such M dwarf interlopers should not contribute to our "excesses" in Figures 1 and 2, if sufficiently dominant, statistical fluctuations might conspire to create a false excess signal, as could *actual* local M dwarf substructure. To assess the influence of M dwarf interlopers, we use a reduced proper-motion diagram (hereafer, RPMD) for luminosity discrimination. A 'proper-motion' estimate, μ, was calculated from the 2MASS-PSR parameter `dist_op`, which gives the displacement between the 2MASS source position and an associated optical source in some published catalogues. We used only `dist_op` measured with respect to USNO-A2.0. This parameter was divided by 50 or 20 yr, for declinations above or below $-30°$, respectively, to take into account the approximate time baseline from the first epoch observations made at Palomar and ESO, respectively. A TriAnd target field was defined by the range $(l, b) = ([105° : 125°], [-18° : -40°])$, corresponding to the area where TriAnd appears strongest. We extract from the 2MASS catalogue all stars having $11.0 < K_S < 12.5$ in the TriAnd and symmetric fields (since this is the magnitude range that has been translated to the TriAnd distances in Fig. 1) and take the difference between the averaged RPMD of the symmetric fields and the TriAnd field RPMD. An example of this extracted RPMD is shown in Figure 3. We have used diagonal Galactic symmetry to construct this particular plot; the other two symmetry tests yield similar results. The RPMD quantity $\mathcal{H}_K$ is given by $\mathcal{H}_K \equiv K_S + 5\log\mu + 5$. Figure 3 shows a residual red giant branch (RGB) down to a red clump at $J-K \sim 0.6$ in the TriAnd RPDM. The theoretical RGB isochrone for [Fe/H] $= -1.0$ (Ivanov & Borissova 2002) gives a reasonable fit to the observed RGB. Nevertheless, figure 3 suggests that some M dwarfs with $J-K_S \gtrsim 0.85$ interlope in the sample, but the number of TriAnd M giants greatly increases with this color selection.

Another feature visible in the RPMD is a significant excess of main sequence turnoff stars with $J-K_S \lesssim 0.40$; the corresponding mean apparent magnitude of these stars is $K_S \approx 12.1$.

The turnoff and M dwarfs are local features that should be located at 500-1000 pc and 150-200 pc, according to typical JHK_S magnitudes for a G0 and M4 dwarf, respectively. Therefore, these features are unrelated to the RGB stars with $J - K_S > 0.90$, since, with $K_S > 11.0$, such RGB stars are located much farther away from the Sun, presuming an average absolute magnitude of $\langle M_{K_S} \rangle \sim -5.5 \pm 1.1$ (Rocha-Pinto et al. 2004, in preparation).

4. Spectroscopy of Triand Stars

A test of the nature of the TriAnd excess comes via the kinematical properties of its constituent stars. We collected spectra for 36 TriAnd and ten Per M giants, as well as 51 spectra of twenty radial velocity standard stars on UT 2003 December 13–18, as part of an ongoing M giant radial velocity program using the B&C Spectrograph on the Bok 2.3 m telescope at Steward Observatory. The spectra cover 7800 Å $< \lambda <$ 9000 Å at $R \sim 3300$. Radial velocity standards were taken from the IAU standard list and from stars in Bettoni & Galletta (2001). Spectral reduction and v_r calculations followed the procedure outlined by Crane et al. (2003). Our internal radial velocity accuracy (~ 8 km s^{-1} among v_r standards) is larger than the 2.7 km s^{-1} achieved by Crane et al. (2003) due to differences in resolution and a slight undersampling of the Bok data compared to Crane et al.'s spectra.

Our observations are summarized in Table 1, where we give, for each star, respectively, its name, Galactic coordinates, Julian day of observation, estimated S/N ratio per pixel at $\lambda \sim 8630$ Å, K_S, $J - K_S$, the mode of the DPDF, heliocentric v_r and its associated error, derived metallicity (see below) and the overdensity to which the star belongs, respectively. Figure 4 summarizes our v_r measurements of TriAnd and Per stars, transformed to the Galactic Standard of Rest, using $\Theta_{\rm LSR} = 220$ km s^{-1}. Only a few TriAnd stars have v_r consistent with being disk M dwarfs. Moreover, most TriAnd stars show a relatively small observed velocity dispersion [$\sigma \sim 19.5$ km/s around a linear fit of the $v_r(l)$ trend (not shown in the plot), after discarding stars deviating by more than 3σ] and have an average velocity (~ 27 km s^{-1}) inconsistent with a circular orbit at $R_{\rm GC} = 30$ kpc assuming a flat Galactic rotation curve. In contrast, Perseus stars have $\langle v_r \rangle = 57$ km/s — i.e. not completely inconsistent with being disk stars; their observed dispersion is $\sigma \sim 20.7$ km s^{-1}. Taking into account an average observed error in v_r for these stars of 10 km s^{-1}, the real velocity dispersion of the TriAnd and Per samples are 17 and 18 km s^{-1}, respectively. The $v_r(l)$ trend found among TriAnd stars does not seem to connect with the Perseus stars, despite our initial expectation that they were part of the same structure. On the other hand, the TriAnd velocity trend *does* fall along that of GASS, suggesting a possible connection, though we stress that the two features are at different distances, with GASS *interior* to

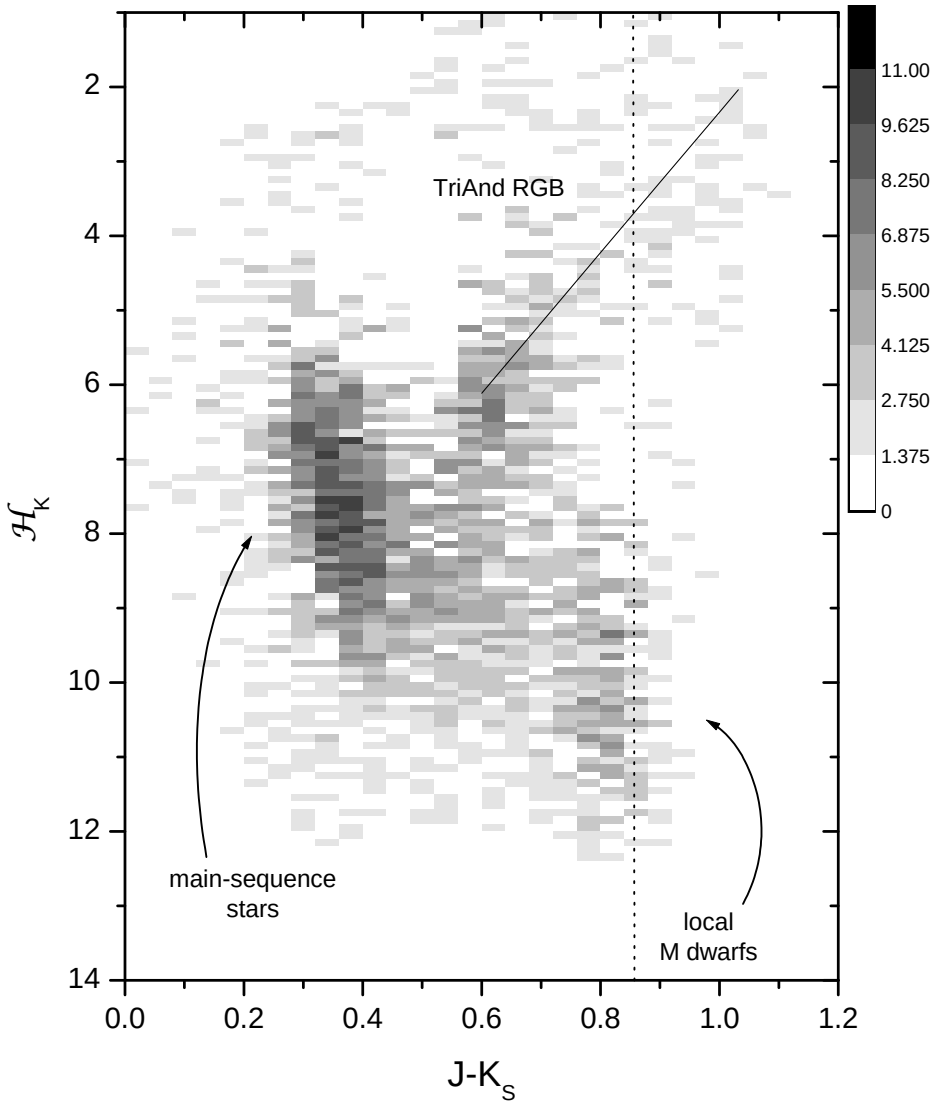

Fig. 3.— Hess-like diagram showing the residual RPMD of stars in the TriAnd field with $11.0 < K_S < 12.5$ after subtracting the field with diagonal Galactic symmetry and discarding stars in all 1 deg^2 bins (and symmetric counterparts) reddened by $E_{B-V} > 0.15$. The color bar scales to $\sqrt{N}$, where N is the number of stars in each diagram cell. The dotted vertical line indicate the original blue color limit used in the discovery of TriAnd and in Figures 1 and 2. A solid line marks the expected locus of the RGB for a population with [Fe/H] $= -1.0$ dex, according to Ivanov & Borissova (2002).

TriAnd (Majewski et al. 2004, in preparation)[1].

The NIR Na I doublet ($\lambda\lambda 8193, 8195$) is a well known index sensitive to $\log g$ and can be used to classify the stars we observed as giants or dwarfs (Schiavon et al. 1997). Six of the stars in Table 1 have red dwarf gravities and two stars have undefined spectra, although they are more likely to be dwarfs than giants. The other stars have red giant spectra, according to the standards given by Schiavon et al. (1997). The red dwarfs are just those stars in the TriAnd longitude range that have v_r closer to the expected local trend in Figure 4. The last column of Table 1 indicates whether the star have dwarf ('D'), giant ('G') or undefined ('U') spectra.

Metallicities were calculated from the same spectra by comparing the sum of three Ca IRT spectral indices for target and standard stars, as explained by Crane et al. (2003). Only spectra with a S/N higher than 30 were used in this calculation. The result is an average metallicity [Fe/H] $= -1.2$, with $\sigma \sim 0.5$ dex, for twenty TriAnd stars. Per stars are more metal poor, with $\langle$[Fe/H]$\rangle \leq -1.5$. Metallicity was not calculated for the stars spectroscopically identified as dwarfs, since our relation between [Fe/H] and the Ca IRT indices was calibrated with M giant standards.

5. Discussion

A remarkable aspect of the TriAnd feature is that it is very diffuse and large. This no doubt conspired to keep it hidden among Milky Way stars, in spite of it being at relatively high ($l \sim 30^\circ$) Galactic latitude. In a companion paper, Majewski et al. (2004) detect the more populous, though still diffuse TriAnd main sequence turn-off, and from the rather constant areal density of these stars calculate a luminous mass of $\sim 1.6 \times 10^6 M_\odot$. These are properties unlike any known Milky Way satellite. If a bound system, TriAnd must be a very massive, but very *dark* satellite. Our calculated velocity dispersion would be consistent with a system having a very large M/L.

Alternatively, with such a low luminous mass, TriAnd could be a largely unbound cloud of stars from a completely disrupted dwarf galaxy. A recent catastrophic disruption could explain a diffuse, apparently coreless but still round configuration, and why the system has not yet stretched into tidal tails — although, such tidal tails would be even *more* diffuse

[1]We have considered the possibility that the TriAnd excess is a false signal due to improper photometric distances assigned to GASS stars. Such stars would need to have an [Fe/H] exceeding +1.0 dex to reduce their distances to that of the foreground GASS stars. But these metallicities are strongly ruled out by the [Fe/H] values calculated for some TriAnd stars in this paper.

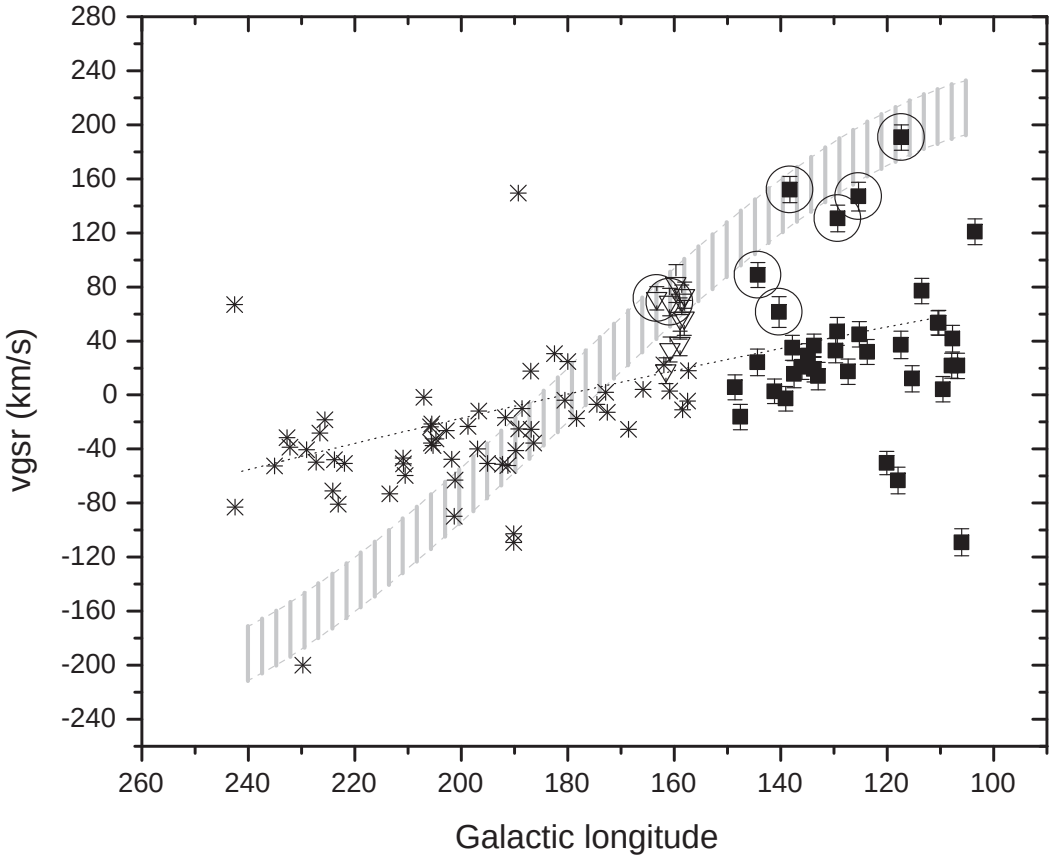

Fig. 4.— Radial velocity of program stars in the Galactocentric Standard of Rest as a function of Galactic longitude. Stars in the TriAnd and Per groups are shown by squares and upside-down triangles, respectively. We also show velocities for GASS stars published by Crane et al. (2003, asterisks). The hatched area is the expected 2σ region for local M dwarfs following a circular orbit with rotation velocity $\Theta_{\rm LSR}$, σ = 10 km s^{-1}, about the Galactic Center, while the dotted curve is for a similar rotational velocity at $R_{\rm GC} = 30kpc$. Stars classified as dwarfs or having undefined classification, according to the presence of strong Na I doublet lines the spectrum, are marked by an open circle.

than the center of the system, and therefore even more difficult to detect. On the other hand, TriAnd may itself *be* tidal debris, perhaps just one higher density part of a longer, but diffuse tidal tail system.

An obvious possibility is that TriAnd is an old piece of the system creating the closer GASS tail, perhaps a different, larger radius orbital wrap of this satellite galaxy. A similar orbital shape might explain the apparent continuous velocity trend from GASS to TriAnd stars seen in Figure 4. The more metal poor content of TriAnd M giants compared to GASS M giants (Crane et al. 2003) would be consistent with the idea that TriAnd is older both in terms of stellar ages and dynamical ages than the inner GASS stars. We plan to address these questions as well as the nature of Per in an upcoming paper.

We acknowledge funding by NSF grant AST-0307851, NASA/JPL contract 1228235, the David and Lucile Packard Foundation, and the generous support from Frank Levinson and Wynnette LaBrosse through the Celerity Foundation.

REFERENCES

Bessell, M. S., & Brett, J. M. 1988, PASP, 100, 1134

Bettoni, D., & Galletta, G. 2001, A&A, 368, 593

Crane, J. D., Majewski, S. R., Rocha-Pinto, H. J., Frinchaboy, P. M., Skrutskie, M. F., & Law, D. R. 2003, ApJ, 594, L119

Girardi, L., Bressan, A., Bertelli, G., & Chiosi, C. 2000, A&AS, 141, 371

Ibata, R. A., Gilmore, G., Irwin, M. J. 1994, Nature, 370, 194

Ibata, R., Irwin, M., Lewis, G., Ferguson, A. M. N., & Tanvir, N. 2001, Nature, 412, 49

Ibata, R. A., Lewis, G. F., Irwin, M. J., & Cambrésy, L. 2002, MNRAS, 332, 921

Ivanov, V. D., & Borissova, J. 2002, A&A, 390, 937

Majewski, S. R., Munn, J. A., & Hawley, S. L. 1996, ApJ, 459, L73

Majewski, S. R. 2003, in New Horizons in Globular Cluster Astronomy, ASP Conf. Proc., Vol. 296, eds. G. Piotto, G. Meylan, S. G. Djorgovski & M. Riello. p. 447

Majewski, S. R., Skrutskie, M. F., Weinberg, M. D., & Ostheimer, J. C. 2003, ApJ, 599, 1082 (M03)

Majewski, S. R., Ostheimer, J. C., Rocha-Pinto, H. J., Patterson, R. J., Guhathakurta, P., Reitzel, D. 2004, in preparation

Newberg, H. J., Yanny, B., Rockosi, C. M., et al. 2002, ApJ, 569, 245 (N02)

Rocha-Pinto, H. J., Majewski, S. R., Skrutskie, M. F., & Crane, J. D. 2003, ApJ, 594, L115 (R03)

Schiavon, R. P., Barbuy, B., Rossi, S. C. F., & Milone, A. 1997, ApJ, 479, 902

Schlegel, D. J., Finkbeiner, D. P., & Davis, M. 1998, ApJ, 500, 525

Willman, B., Governato, F., Dalcanton, J. J., Reed, D., & Quinn, T. 2004, astro-ph/0403001

Table 1. Data for program stars.

name	l	b	JD	S/N	K_S	$J-K_S$	d (kpc)	v_r (km/s)	ϵ_{v_r}	[Fe/H]	group	Spec.
2MASSX J00091797+3630588	113.56	−25.59	2452987.678	25	9.86	1.20	25.06	−110.7	9.6	−1.2	TriAnd	G
2MASSX J00191095+3348239	115.30	−28.59	2452987.688	60	10.06	1.17	25.28	−167.3	9.7	−1.0	TriAnd	G
2MASSX J00253106+3828397	117.38	−24.11	2452989.630	35	12.08	0.92	25.51	+8.0	9.6	···	TriAnd	D
2MASSX J00273574+3504151	117.43	−27.55	2452990.631	25	12.04	0.96	29.69	−137.9	10.2	−1.3	TriAnd	G
2MASSX J00282905+3753390	117.95	−24.76	2452990.621	40	11.41	1.03	28.04	−245.1	10.0	−0.8	TriAnd	G
2MASSX J00373441+4042425	120.10	−22.08	2452989.643	35	11.42	1.01	26.48	−210.4	8.5	−0.8	TriAnd	G
2MASSX J00545179+3510599	123.72	−27.68	2452990.643	35	11.50	0.98	24.46	−130.9	9.4	−1.1	TriAnd	G
2MASSX J01002299+2957238	125.24	−32.88	2452987.697	50	9.72	1.18	22.30	−107.7	9.6	−0.8	TriAnd	G
2MASSX J01023690+3735148	125.38	−25.23	2452991.629	40	11.91	0.94	25.28	−17.1	10.7	···	TriAnd	D
2MASSX J01110387+3553193	127.39	−26.81	2452987.704	30	9.28	1.27	24.69	−140.5	9.5	< -1.5	TriAnd	G
2MASSX J01172688+3218515	129.29	−30.24	2452990.653	25	12.03	0.97	30.38	−14.3	9.8	···	TriAnd	U
2MASSX J01214158+3635505	129.68	−25.88	2452987.709	50	10.65	1.06	22.53	−121.5	9.1	−0.9	TriAnd	G
2MASSX J01234407+4131080	129.40	−20.95	2452989.654	30	11.77	0.94	24.32	−116.5	9.6	−0.6	TriAnd	G
2MASSX J01372969+3719375	132.99	−24.64	2452989.672	35	11.29	1.00	23.50	−133.2	10.3	−1.2	TriAnd	G
2MASSX J01403652+3649067	133.77	−25.02	2452987.717	25	11.08	1.02	23.58	−107.0	8.6	−0.1	TriAnd	G
2MASSX J01425641+3851201	133.79	−22.93	2452987.725	30	10.73	1.07	23.81	−127.9	9.4	−0.8	TriAnd	G
2MASSX J01450678+3623258	134.85	−25.24	2452987.732	20	10.65	1.17	32.87	−105.3	9.3	−1.1	TriAnd	G
2MASSX J01513509+2339258	140.29	−37.18	2452990.666	20	12.24	0.94	29.69	−43.3	11.2	···	TriAnd	D
2MASSX J01561741+4044275	135.98	−20.48	2452989.662	30	11.47	1.00	26.33	−122.5	9.5	−1.4	TriAnd	G
2MASSX J01581477+1827407	144.32	−41.62	2452991.644	25	12.07	0.92	25.97	−5.7	9.6	···	TriAnd	D
2MASSX J02001321+3547225	138.28	−25.02	2452987.739	30	10.99	1.08	28.18	+21.0	9.7	···	TriAnd	D
2MASSX J02044137+4059528	137.53	−19.79	2452987.748	40	11.11	1.00	22.39	−124.5	10.1	−0.7	TriAnd	G
2MASSX J02075025+4201519	137.79	−18.63	2452987.758	30	9.92	1.20	25.97	−105.1	9.3	< -1.5	TriAnd	G
2MASSX J02133023+4131328	139.02	−18.77	2452989.685	30	11.24	1.05	27.81	−139.1	9.2	< -1.5	TriAnd	G
2MASSX J02195064+3850488	141.21	−20.87	2452991.658	25	11.95	0.93	25.51	−125.7	9.0	−0.2	TriAnd	G
2MASSX J02222634+3216028	144.42	−26.78	2452990.712	30	11.41	1.00	24.91	−77.4	10.5	−1.2	TriAnd	G
2MASSX J02481130+3650021	147.54	−20.40	2452989.695	25	9.81	1.19	23.86	−124.5	9.5	< -1.5	TriAnd	G
2MASSX J02541392+3702586	148.57	−19.64	2452990.725	18	11.80	0.94	24.41	−98.6	9.2	−0.8	TriAnd	G
2MASSX J03244829+3030073	158.06	−21.72	2452989.701	15	10.48	1.12	25.65	+6.5	9.4	−1.2	Per	G
2MASSX J03245531+3026213	158.12	−21.75	2452989.712	20	10.73	1.06	23.13	−9.3	13.2	< -1.5	Per	G
2MASSX J03283560+3042261	158.62	−21.06	2452991.701	15	11.49	1.02	28.18	+4.0	11.1	−1.0	Per	G
2MASSX J03290508+3022080	158.93	−21.27	2452989.730	50	8.29	1.45	29.85	−29.3	9.2	−1.1	Per	G
2MASSX J03303497+3050191	158.90	−20.70	2452990.737	12	11.62	0.99	26.48	−4.0	14.2	< -1.5	Per	G
2MASSX J03355851+3107296	159.69	−19.76	2452991.715	15	11.42	0.97	23.21	+15.2	12.3	< -1.5	Per	G
2MASSX J03415347+2954439	161.55	−19.90	2452987.766	30	10.34	1.15	26.84	−40.4	9.7	−1.4	Per	G

Table 1—Continued

name	l	b	JD	S/N	K_S	$J-K_S$	d (kpc)	v_r (km/s)	ϵ_{v_r}	[Fe/H]	group	Spec.
2MASSX J03443920+3144508	160.79	−18.11	2452987.775	25	10.13	1.16	25.28	−26.4	9.5	−1.4	Per	G
2MASSX J03453551+3156257	160.82	−17.83	2452989.741	20	11.28	1.01	24.55	+6.9	10.0	···	Per	U
2MASSX J04021237+3209591	163.41	−15.33	2452989.755	20	11.96	0.93	25.14	···	···	< -1.5	Per	G
2MASSX J04043600+3343381	162.68	−13.85	2452991.856	20	11.91	0.94	25.74	···	···	< -1.5	Per	G
2MASSX J04063385+3316474	163.31	−13.89	2452991.871	30	11.42	0.96	22.30	+14.0	10.6	···	Per	D
2MASSX J23280198+3312451	103.50	−26.49	2452987.662	20	11.24	1.02	25.51	−79.1	9.8	−0.6	TriAnd	G
2MASSX J23333834+3909235	106.85	−21.27	2452987.639	25	10.60	1.07	22.62	−180.8	9.5	−0.1	TriAnd	G
2MASSX J23382512+3927458	107.89	−21.27	2452990.587	30	11.64	0.98	26.39	−181.6	9.4	−1.4	TriAnd	G
2MASSX J23413614+3143111	105.99	−28.84	2452990.600	40	11.17	1.04	26.48	−300.2	10.0	−1.4	TriAnd	G
2MASSX J23485366+3144486	107.70	−29.27	2452990.610	30	11.30	1.04	27.89	−147.6	9.8	−0.9	TriAnd	G
2MASSX J23490540+4057312	110.43	−20.39	2452989.603	25	11.11	1.02	23.35	−145.4	9.1	−1.1	TriAnd	G
2MASSX J23534927+3659173	110.32	−24.47	2452989.612	25	11.02	1.07	26.84	−142.3	9.4	−1.4	TriAnd	G
2MASSX J23583475+3009356	109.55	−31.34	2452989.623	45	10.08	1.18	26.33	−178.5	9.3	< -1.5	TriAnd	G